JOURNAL OF THERMOPHYSICS AND HEAT TRANSFER
Vol. 23, No. 1, January–March 2009

# Chemical Kinetic and Radiative Simulations for Titan Atmospheric Entry

C. Rond* and P. Boubert†
*Université de Rouen, 76801 St. Etienne du Rouvray, France*

DOI: 10.2514/1.36918

**Numerical simulations have been carried out to reproduce thermochemical and radiative processes behind a strong shock wave for Titan-like mixtures. The chemical nonequilibrium is modeled by a two-temperature kinetic code and the corresponding Boltzmann radiation is estimated by a line-by-line calculation. Assumptions of the thermochemical model are detailed because of their significant influence as we highlight for the thermodynamic data at high temperature. The study of parameter sensitivity confirms the effect of the chemical kinetic scheme, the effect of $CH_4$ proportion variation, and the pressure influence. The comparison with experiments carried out on a TCM2 shock tube is performed. Spectra, flux, and temperature time evolutions show a quite good agreement for intensity but an approximate simulation of relaxation. Finally, the numerical results are compared to two more improved models which better simulate the intensity and the decay rate of the CN violet system emission. All of the results invalidate the Boltzmann assumption and so speak in favor of the development of a collisional radiative model for an accurate description. Nevertheless, the two-temperature model detailed in this paper provides a good estimation of the CN emission so it could be efficient for coupling with computational fluid dynamics codes.**

## Nomenclature

| | | |
|---|---|---|
| $a_v$ | = | absorption coefficient |
| $C_p$ | = | specific heat capacity at constant pressure |
| $D$ | = | diameter of the shock tube |
| $e$ | = | specific internal energy |
| $H$ | = | enthalpy |
| $i$ | = | subscript for species |
| $i_v$ | = | emission coefficient |
| $K_{\text{eq}}$ | = | equilibrium constant |
| $k_b$ | = | backward rate coefficient |
| $k_f$ | = | forward rate coefficient |
| $L_v$ | = | spectral intensity |
| $\hat{M}$ | = | molecular weight |
| $m$ | = | subscript for molecules |
| $P$ | = | pressure |
| $p_i$ | = | initial pressure |
| $p_s$ | = | postshock pressure |
| $\hat{R}$ | = | universal gas constant |
| $S$ | = | entropy |
| $T$ | = | rotational-translation temperature |
| $T_{\text{sh}}$ | = | translation temperature just behind the shock wave |
| $T_v$ | = | electron-electronic-vibrational temperature |
| $T_{v,\text{sh}}$ | = | vibrational temperature just behind the shock wave |
| $u$ | = | fluid velocity |
| $v$ | = | subscript for vibrational term |
| $v_s$ | = | shock wave velocity |
| $X_{\text{CN}}$ | = | CN molar fraction |
| $y$ | = | mass fraction |
| $\nu$ | = | stoichiometric coefficient |
| $\rho$ | = | density |
| $\tau$ | = | relaxation time |
| $\mathbf{\Phi}$ | = | intensity of the radiative flux |
| $\Omega^{\text{VT}}$ | = | vibration-translation exchange term |
| $\acute{\omega}$ | = | rate of production |

Received 30 January 2008; revision received 13 July 2008; accepted for publication 13 July 2008. 

*Postdoctoral Student; rond@coria.fr.
†Assistant Professor; boubert@coria.fr.

## I. Introduction

AFTER a seven-year interplanetary journey and two orbits aboard the Cassini orbiter, the Huygens probe was released on 25 December 2004. Three weeks later, it reached the upper layer of Titan's atmosphere with a speed of 6 km/s and landed softly after a parachute descent of 2.28 h with a speed slightly less than 5 m/s [1]. Scientific objectives for the Cassini–Huygens mission were numerous [2,3], for example, to determine atmospheric composition, investigate energy sources for atmospheric chemistry, determine properties of the surface, and deduce internal structure.

One of the main technical phases of this mission was the Huygens entry into Titan atmosphere. During the descent, the heat shield was expected to receive a strong radiative flux produced in the bow shock layer. Previous studies [4,5] predicted that the emission is mainly caused by the violet system of CN ($B^2\Sigma^+ \rightarrow X^2\Sigma^+$) with lower contributions from the CN red ($A^2\Pi \rightarrow X^2\Sigma$) and $C_2$ Swan ($d^3\Pi \rightarrow a^3\Pi$) systems. Indeed, because of the quite low energy and the short lifetime of its first excited states and because of its relevant production, the CN radical is known to be a strong radiator, even for other atmospheric entries such as Mars or Venus, and a major species due to the fast dissociation of $CH_4$ behind the shock wave. At hypersonic flight speeds, because of the high enthalpy flow, the shock layer around the vehicle is the seat of internal mode relaxation, dissociation, and ionization leading to the nonequilibrium state of the gas. Considerable effort has been expended over the last 25 years to compute this phenomenon numerically during Titan entry, beginning with Park who questioned the equilibrium assumption [4] and proposed as an answer a two-temperature (2-$T$) modeling [6] for the kinetic calculation. Up to now his theory has been widely reused by other authors [7–9] and has also served as a basis to develop more detailed models such as 3-$T$ calculations [5,10] or collisional radiative models [11,12]. A model which takes into account the collisional excitation of molecules, especially CN, is of interest to predict thermochemical mechanisms precisely. But because of its low calculation time cost the 2-$T$ model is preferable to perform calculations efficiently coupled with flowfield [13] or three-dimensional radiative transfer [14].

Few kinetic models have been developed for $CH_4$–$N_2$–Ar chemistry. Two of them are mainly used for 2-$T$ physical theory: the Nelson model [9] and the Gökçen model [7]. Nelson originally proposed a 22-reaction kinetic scheme but Gökçen pointed out that it was incomplete. He proposed a new chemical kinetic model for a Titan-like mixture (a detailed one with 74 reactions and a simplified one with 35 reactions) and made a comparison with a sample case [7].

The purpose of the present study is to investigate the chemical kinetic model of Gökçen [7] for a 2-$T$ calculation. A thermochemical code is developed based on Park's 2-$T$ theory [6] and the corresponding results are compared with Gökçen's model in order to highlight the influence of the physical model. In particular, there are still many unknown thermodynamic parameters for high-temperature real gases. A radiative code following the thermochemical calculation is necessary to compare numerical and experimental results. A line-by-line algorithm has been developed including most of the systems present in the planetary atmosphere. A careful study is performed on the different parameters influencing the radiative flux, the gas composition, the pressure, and the shock velocity. Consequences on the emission are deduced from the thermochemical data evolution. We also develop a basic comparison between the Nelson and the Gökçen kinetic schemes and justify the choice of Gökçen's model. Accuracy and validity of such calculations are to be verified, so it becomes desirable to make comparisons with experiments. Test results used are mainly those obtained on the TCM2 shock tube in Marseilles and were the subject of a previous paper [15]. Furthermore, experimental results proposed by Bose et al. [11] were also compared to our simulations. Finally, through these two sets of experimental results, the 2-$T$ model is compared with improved calculations developed by Bose et al. [11] and Hyun et al. [16].

## II. Numerical Modeling

The numerical analysis developed in this work deals with the simulation of the thermochemical and radiative evolution of the gas behind a normal shock wave. The objective of the modeling is to propose an approximate computational approach that could be implemented in CFD flowfield codes for aerothermal analysis. For this reason, two independent codes are developed: a chemical kinetic code for the evolution of one-dimensional thermodynamic properties and a radiative code to estimate the corresponding heat flux parameters.

On the one hand, this two-step numerical method presents the advantage of being simple with a low time cost, but on the other hand, it does not take into account the coupling between chemistry and radiation.

### A. Thermochemical Model

Input data for the code, such as pressure, temperature, and mixture composition, are set using test cases or experimental conditions close to Titan entry parameters [17]. The calculation is initialized assuming that the thermochemical state of the gas is frozen through the shock, whereas thermodynamic properties ($P$, $T$, $\rho$, and $u$) are obtained with the perfect gas shock jump conditions (Rankine–Hugoniot equations). From these new values of pressure, temperature, density, and velocity of the mixture just behind the shock, the downstream flowfield is then computed by solving one-dimensional Euler equations temporally.

The kinetic code developed in the frame of this work is based on a 2-$T$ theory developed by Park [6]. This model implies three assumptions: 1) It is generally admitted, whatever the thermochemical model used, the rotational and the translational temperatures of the heavy particles are equal, and this variable is noted as $T$. This statement is based on the knowledge that energy exchange between the translational and rotational modes is very rapid [10] because collisions are very efficient for high pressures. 2) Calculations on other gases [12,18] show that the vibrational temperature evolutions of the different molecular species are very close to each other. So the coupling among the vibrational modes of the molecules can be considered strong and only one vibrational temperature $T_v$ is defined. 3) Finally, the electron temperature could be easily considered strongly coupled with the vibrational temperature of molecules, because inelastic collisions between electrons and molecules are mainly responsible for vibrational excitation [8]. Furthermore, electronic excitation of particles equilibrates quickly with the electronic ground state through collisions with electrons [10]. So the 2-$T$ model defines an electron–electronic–vibrational temperature [19] ($T_v$). These three statements imply the assumption of Boltzmann distribution for each internal mode. But the high enthalpy flow behind the shock wave leads the electronic mode to be out of Boltzmann equilibrium.

The 21 species included in the chemical model are $C_2$, C, $N_2$, N, CH, H, CN, $CH_4$, $CH_3$, $CH_2$, CH, $H_2$, $CN^+$, $N^+$, $N_2^+$, $C^+$, $H^+$, Ar, $Ar^+$, $e^-$, and HCN.

The physical model is based on the works of Gnoffo et al. [20] and Park [21]. The gas is considered as an ideal mixture of perfect gases. The specific energy of each species $e_i$ takes into account the contribution of the different internal modes and the energy of formation. Rotational and vibrational energy modes are assumed to be in a Boltzmann equilibrium, respectively, using the rigid rotor and harmonic oscillator models.

The vibrational relaxation model involves vibration–translation exchange, which is modeled using a Landau–Teller relaxation formula. The correction terms are given by Park [22] to take into account the limiting value of the cross section and the diffusive nature of vibrational relaxation as a result of the high temperature. The relaxation time follows the Millikan–White formula [23] including the first Park correction [19]. Because of the lack of data, polyatomic molecules are taken into account as diatomic molecules.

The forward $k_f$ and backward $k_b$ rate coefficients for each reaction are expressed following an Arrhenius formulation. Backward rate coefficients are determined using the equilibrium constant according to the microreversibility principle $k_b(T) = k_f(T)/K_{\text{eq}}(T)$. Reaction rate temperatures depend on the nature of the associated process [12]. In particular, the governing temperature for all dissociation reactions is assumed to be $\sqrt{TT_v}$ [21] to take into account the preferential removal of highly vibrational states in dissociation [24].

We have calculated the equilibrium constants using the minimized Gibbs free energy approach [25]. The values of the thermodynamic data ($C_p$, H, S) for the species have to be known for a wide range of temperatures [0–50,000] K. NASA's CEA (Chemical Equilibrium with Applications) [26] computer program provides this information for the 21 species named previously, but for polyatomic molecules, the CEA-NASA data are available only up to 6000 K. Capitelli et al. [27] calculate the thermodynamic properties of high-temperature Mars-atmosphere species from 50 to 50,000 K, but the hydrogenated species are not included. Because these available data sets are incomplete, we have calculated the thermodynamic properties of Titan atmospheric species for temperatures up to 50,000 K, using classical methods [28]. The resulting temperature variations of the thermodynamic data are compared to those of CEA-NASA and Capitelli et al. (Fig. 1). For most species, agreement is correct for low temperatures whereas the discrepancies reach a factor of 2 for high temperatures. Actually when trying different sets of values for thermodynamic data, we observed that thermochemical results are very sensitive to the method of high-temperature data estimation. The lack of information at high temperatures is a real problem in estimating the thermodynamic data because relaxation of the gas is strongly dependent on the state of high enthalpy just behind the shock.

As stated previously, the physical model is based on a 2-$T$ approach. The chemical kinetic scheme chosen to perform our simulations is the Gökçen reduced kinetic scheme [7]. However, this model was conceived using a single-temperature calculation. The comparison between our calculations and the Gökçen results [7] highlights the influence of the physical model. Indeed, for the same initial conditions and kinetic scheme, we can observe some discrepancies between the time evolution of mole fractions, particularly for N, CN, $H_2$, $CH_2$, $CH_3$, and $CH_4$. The relaxation of molecules, in particular polyatomic ones, is slower for the 2-$T$ model because the dissociation is mainly controlled by the average temperature $\sqrt{TT_V}$ which is lower than the equilibrium temperature used in the 1-$T$ model. The equilibrium value of mole fractions presents significant differences; for example, the CN mole fraction estimated by the 2-$T$ calculation is 150% higher than the 1-$T$ prediction. Furthermore, charged species computations present a 3-order-of-magnitude divergence because the two-temperature model

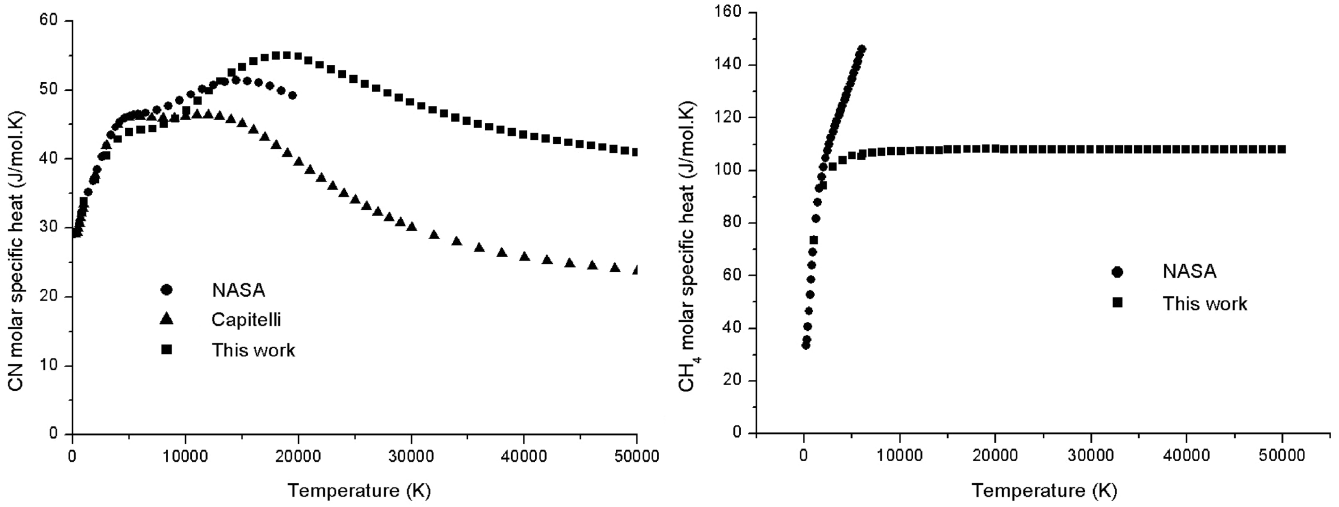


**Fig. 1 Calculated molar specific heat in relation to temperature for CN and $CH_4$.**

underestimates the temperature of the electrons in comparison with the Gökçen single-temperature model. And so associative ionization reactions, which are the main ionizing processes behind a strong shock wave, are less significant and thus the computed ionization level is lower.

### B. Radiative Model

The radiative code PASTIS is used both to extract and process spectra and time profiles from experimental charge-coupled device (CCD) images [15] and to estimate the radiation corresponding to the chemical kinetic calculation. The code is based on a line-by-line radiation calculation assuming Boltzmann distributions for the internal modes. A temperature may be defined for each energy storage mode for each molecule; however, in the radiative code, only one rotational temperature, one vibrational temperature, one electronic excitation temperature, and the kinetic temperature of heavy particles are defined. Obviously in this study, radiative calculations are performed using two temperatures to be consistent with the thermochemical model.

As shown in previous studies [9], the experimental results [15] attest that the CN violet (B-X) system is the most radiative system in the near [UV-IR]; therefore, the description of its mechanisms has been deeply investigated. It is also necessary to know the spectral distribution of the two other experimentally observed systems: the CN red (A-X) system and the $C_2$ Swan (d-a) bands, and also other systems such as the CH (A-X), (B-X), and the (C-X) systems, on the one hand, and the CN LeBlanc (B-A) system, on the other hand. The code is also capable of calculating the radiation from atoms and most of the diatomic molecule systems present in planetary atmospheres but not the vacuum UV emission of the CN systems. The radiative code PASTIS has been validated thanks to spectra obtained in flames and plasma jets [29].

Our code has been developed to calculate spectra from 100 to 1200 nm with a good level of accuracy. No hypothesis has been made about the energy level of CN and $C_2$. Vibronic term values and rotational constants obtained from experiments, when they were available, have been preferred to Dunham expansion. When experimental data were not available, constants have been extrapolated.

Considering the pressures behind the shock wave (from $2.10^4$ to $3.10^5$ Pa), self-absorption has to be considered in the calculations. Bose et al. modeling [11] demonstrates the importance of nonlocal absorption. To simulate the radiative flux recorded by a spectrometer, the radiative transfer equation may be solved along the line of sight. Moreover, in our first approximation we neglected the boundary layer thickness, and we considered that the radiative medium was homogeneous. In this case, the radiative transfer equation is solved analytically:

$$L_v = \frac{i_v}{a_v}(1 - e^{-a_v D})$$

The code models pressure and Doppler broadenings in a Voigt line shape. The numerical spectral resolution has to be high enough to correctly describe the line shape. Calculations at different numerical resolutions have shown that in the near-ultraviolet and visible ranges, a resolution equal to 1000 points/nm is sufficient.

The radiative code PASTIS uses the results of chemical kinetics codes as input (time evolution of temperatures and densities) but the calculated radiative heat flux is not used in the chemical kinetics code as a power loss in this study.

## III. Sensitivity Study

This part of our study is based on a set of experiments carried out in the TCM2 shock tube facility made according to the Stalker principle. The specified description of the installation and the associated measurement techniques are developed in [15]. The diagnostic apparatus, a monochromator and a streak system, is based on time-resolved emission spectroscopy, and so the information extracted from the experiments is of two kinds: temporal and spectral. The experimental data are calibrated and the comparisons are done in absolute units ($W/m^2$ sr).

### A. Experimental Campaign

The different tests carried out may be classified into three groups corresponding to the three values of initial pressure for a relatively constant velocity. They are presented in Table 1 with initial pressure (measured), postshock pressure (calculated), and shock velocity (measured). The values presented are averages for the whole set of tests done.

For both lower pressure conditions, experiments have been carried out for four different mixtures with variable proportions of nitrogen, methane, and argon. They are presented in Table 2. The composition will be noted ($\%CH_4/\%Ar/\%N_2$) as follows.

This experimental campaign begins to answer some questions concerning the nature of the parameters influencing the radiative flux. Considering the absolute value of the flux density and the shape

**Table 1 The three test conditions. Postshock pressures are obtained thanks to the classical Rankine–Hugoniot equation applied to the shock front**

| $p_i$, Pa | $p_s$, Pa | $v_s$, km/s |
|---|---|---|
| 1100 | $30 \times 10^4$ | 5.3 |
| 200 | $8 \times 10^4$ | 5.5 |
| 45 | $2 \times 10^4$ | 5.5 |

**Table 2 Composition of studied mixture in %. For each molecule the second column gives the results of the analysis made by the gas manufacturer**

| | $CH_4$ | Ar | $N_2$ |
|---|---|---|---|
| TCM2 classical | 3 *(2.96)* | 5 *(5.02)* | 92 *(92.02)* |
| Yelle et al. [17] nominal | 3 *(2.93)* | 2 *(2.15)* | 95 *(94.92)* |
| Yelle et al. [17] minimal | 5 *(5.06)* | 0 | 95 *(94.96)* |
| Yelle et al. [17] maximal | 1 *(1.00)* | 10 *(10.30)* | 89 *(88.70)* |

of the profile, it was not possible to conclude a significant influence of the gas composition on CN emission. Two main pressure effects on the evolution of the emission behind the shock front are observed: the total radiative flux density increases with the pressure of the test gas in the shock tube and the lower the initial pressure, the higher the nonequilibrium radiation. These results are based on the assumption that the approximate reproducibility of the experimental conditions ($p_i$ and $v_s$) from one run to another has no influence.

The numerical study proposed in this work is derived from these experimental results. The objectives are to compare numerical predictions with experimental observations and also to confirm the lack of influence from differences in experimental conditions between two runs. For these reasons, the computations are composed of two kinds of simulation. The first one studies the influence of slight fluctuations in different parameters such as gas composition, shock velocity, and initial pressure; the second one investigates the consequences of large variations of those parameters. Initial conditions used for the calculations are chosen to be close to the experimental ones and are presented in Table 3.

### B. Kinetic Model Discussion

First, it is interesting to test the influence of the chemical kinetic model on calculations. The improvement introduced by the use of Gokçen's more detailed kinetic mechanism compared to Nelson's short model has to be confirmed in a 2-$T$ calculation.

Nelson's kinetic scheme used for Gökçen's work [7] contains ionization reactions occurring with electrons (Nelson-$e^-$), whereas Nelson et al. [9] proposed the same ionization reactions occurring with a third body (Nelson-$M$). As electrons are far from being the main species in a gas behind a strong shock wave (ionization level $\leq 10^{-4}$), this change of colliding partner in ionization reactions has an influence on the chemistry. Figures 2b and 2c present, respectively, time evolution of species mole fractions using Nelson-$e^-$ and Nelson-$M$ kinetics. There are significant differences; as expected, mole fractions of $N^+$, $C^+$, and $H^+$ are higher with the Nelson-$M$ scheme because the number of colliding partners for ionization reactions is greater, but there is no meaningful influence on the N, C, and H mole fractions. We also note a modification on the level and evolution of other species mole fractions such as CH, NH, $H_2$, $CH_2$, and molecular ions. This consequence may be an indication of preferential reaction processes in the Nelson scheme as follows:

$$CH + M = C + H + M$$

$$CH_2 + M = CH + H + M$$

$$NH + M = N + H + M$$

$$H_2 + M = H + H + M$$

$$H_2 + C = CH + H$$

For the comparison between the Gökçen and the Nelson-$e^-$ kinetic schemes (Figs. 2a and 2b), we note as did Gökçen [7] some significant differences concerning the level of charged species, hydride species, and also C and N. But contrary to Gökçen's results, the CN mole fraction was the same.

However, Gökçen's model includes important species and reactions for methane decomposition and CN formation. Moreover, the reaction rates used are updated from the current literature values; hence this chemical scheme is chosen in the following work.

### C. Influence of Small Variations

The results presented in this part are of great interest for the comparison between experiments and computations. The objective is to free the experimental results from the uncertainty of the experimental conditions. Within the framework of our experimental campaign on TCM2 [15] we highlighted the approximate reproducibility between runs. Measurement results depend greatly on the influence of these experimental fluctuations. The computations presented in this part will allow us to quantify the consequences of the experimental uncertainties on the radiative flux.

#### 1. *Gas Composition*

The simulations using compositions A, B, C, E, G, and H confirm the experimental observations that there is no significant effect of the gas composition on both intensity and relaxation of the radiative time evolution. The modifications of the nitrogen percentage tested are weak at only about 10% of the nitrogen concentration. The $N_2$ proportion has no major influence on CN emission. The radiative fluxes corresponding to compositions H, G, and E do not present significant discrepancies. The difference appears only for the equilibrium part and is estimated at about 20% between compositions E and H. Nevertheless, the imposed variations of the $CH_4$ proportion are not weak because here the percentage of $CH_4$ is divided by almost a factor of 2.

In summary, for the fixed conditions we do not observe modifications of the radiative flux by changing the $N_2$ percentage up to 10% and $CH_4$ percentage up to a factor of 2.

#### 2. *Pressure*

There is a prefilling uncertainty on the initial pressure in the shock tube that is independent of the pressure level and equal to 8 Pa. So we decided to input a variation of 20% to $P_A$, $P_B$, and $P_C$ to study the weak fluctuation of the initial pressure on the radiative flux. We observe that the lower the pressure, the lower the emission. But this variation is negligible because the flux modifications, whatever the nonequilibrium or equilibrium regions, is only 5%.

**Table 3 Fixed conditions used for numerical investigations on the study of sensitive parameters**

| Composition of studied mixture in % ($p_i = 50$ (Pa); $v_s = 5.5$ km/s) | | | | Pressure in Pa (3/5/92; $v_s = 5.5$ km/s) | | | Velocity in km/s (3/5/92; $p_i = 200$ Pa) | |
|---|---|---|---|---|---|---|---|---|
| | $CH_4$ | Ar | $N_2$ | | $p_i$ | $p_s$ | | $v_s$ |
| Compo A | 3 | 7 | 90 | $P_A$ | 50 | $1.42 \times 10^4$ | $V_A$ | 5 |
| Compo B | 3 | 4 | 93 | $P_B$ | 200 | $5.7 \times 10^4$ | $V_B$ | 5.5 |
| Compo C | 3 | 0 | 97 | $P_C$ | 1000 | $28.5 \times 10^4$ | $V_C$ | 6 |
| Compo D | 1.5 | 3.5 | 95 | | | | | |
| Compo E | 3 | 2 | 95 | | | | | |
| Compo F | 0.1 | 4.9 | 95 | | | | | |
| Compo G | 4 | 1 | 95 | | | | | |
| Compo H | 5 | 0 | 95 | | | | | |

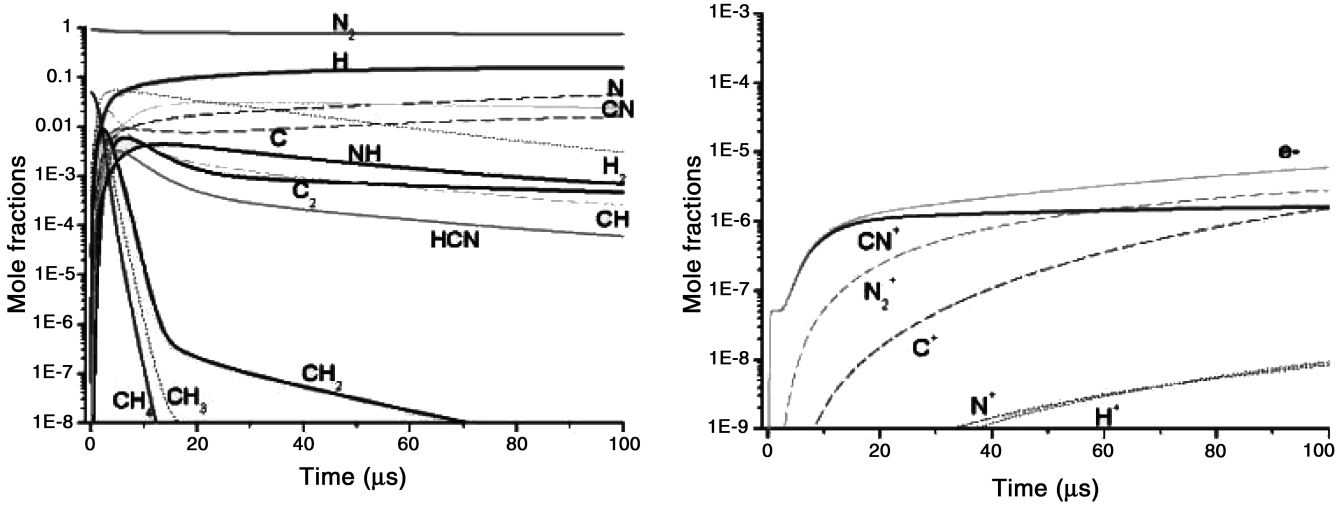


a) Gorkçen reduced kinetic scheme

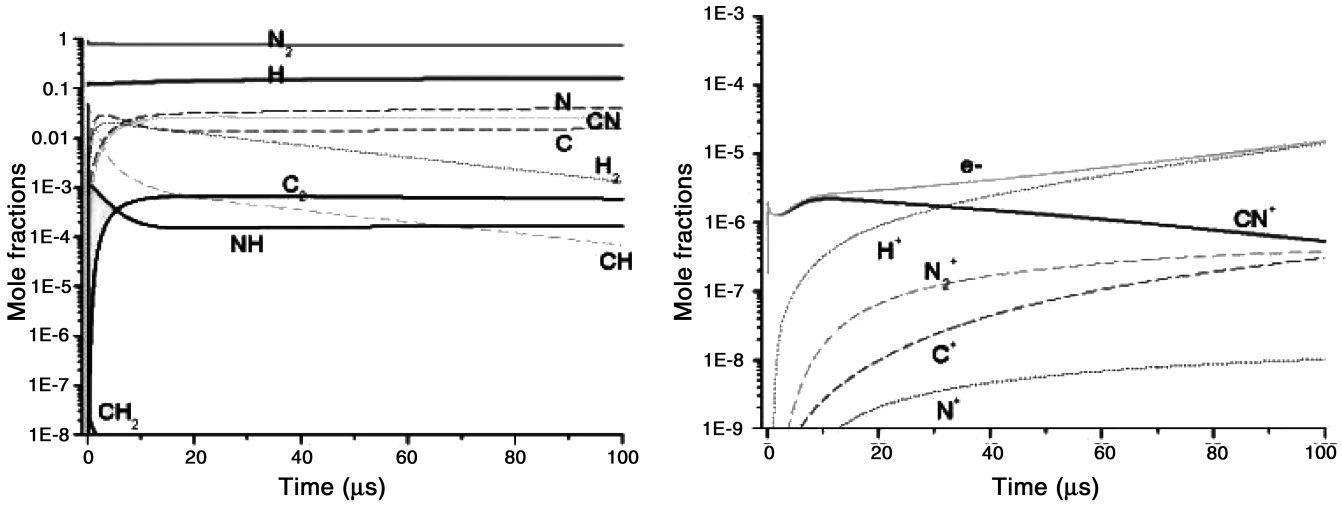


b) Nelson-e kinetic scheme

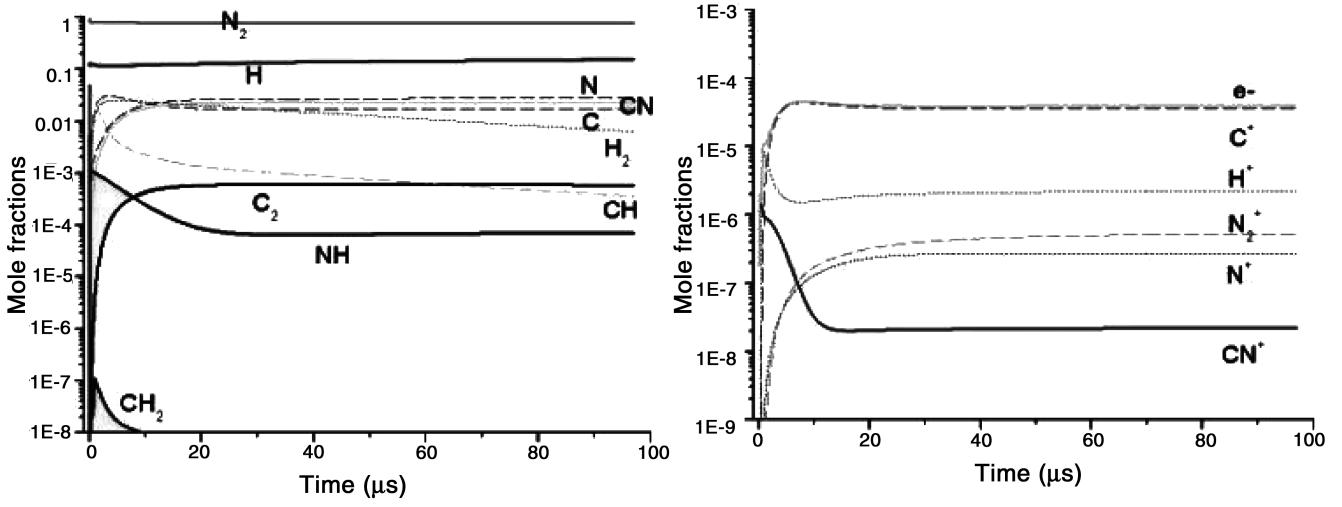


c) Nelson-M kinetic scheme

**Fig. 2 Time evolutions of mole fractions behind a shock wave ($p_1 = 0.1$ torr, $T_1 = 300$ K, $u_1 = 6.3$ km/s, 5% $CH_4$ in $N_2$) using a) the Gökçen reduced scheme, b) the Nelson-*e* scheme, and c) the Nelson-*M* scheme.**

*3. Shock Velocity*

With respect to the general problem of atmospheric entries, the velocity of the vehicle and the angle of attack are important parameters for aerodynamic calculation. Their values can be modified during the journey to adjust the trajectory. Furthermore, experimentally, the shock velocity is very sensitive to some technical parameters which are difficult to control, as, for example, the opening pressure of the membranes. Thus the influence of the velocity is of interest to predict the consequences of such changes on the radiative flux.

We note that increasing the velocity by 20% causes the growth of the nonequilibrium peak by about 10%, with no significant effect on the relaxation and the equilibrium flux. And so we can conclude that the influence is negligible.

Whatever the gas composition, the pressure and the shock velocity, small variations in these parameter values do not produce significant modifications on the radiative flux. The variation of the gas composition, the experimental uncertainty, and the approximate reproducibility do not have a major consequence on the radiative flux. Despite experimental variations, comparisons between runs are relevant.

### D. Influence of Large Variations

Obviously, if the modifications of the parameters are greater, the consequences are most likely to be more significant. But the study of large variations of the parameters has to be realistic, that is, coherent for the problems to be linked to Titan entry. For this reason a large variation in the shock velocity is not expected because the vehicle velocity during the entry phase is close to 5 or 6 km/s. Furthermore, the atmospheric composition is quite well known with the $N_2$ proportion uncertainty lower than 10%. On the other hand, $CH_4$ percentage and initial pressure are parameters that can present large variations. Their influences are studied in this part.

#### 1. $CH_4$ Proportion

Here, the imposed variations of the $CH_4$ proportion are up to a factor of 10 between compo D and compo F, so the influence on the radiative flux becomes nonnegligible (Fig. 3a); the decrease of the $CH_4$ fraction causes the falloff of the radiative flux intensity by about a factor of 5 in the nonequilibrium region and a factor of 10 in the equilibrium region. In this case, the increase in the $CH_4$ percent has no considerable influence on temperatures (rise of 10%) but causes rise of the CN mole fraction level up to a factor of 20 (Fig. 3b). These results have been observed whatever the pressure (50 or 200 Pa). The $CH_4$ proportion in the compo F mixture is very small. In this extreme case the amount of formed CN is obviously low and so the radiative flux is not important.

#### 2. Pressure

Figure 4a illustrates the important role of pressure on the radiative flux. The rise of the initial pressure causes the increase of the emission, in nonequilibrium as well as in equilibrium regions, but also a faster relaxation.

Both the corresponding time evolutions of vibrational temperature and CN mole fraction are responsible for these changes. Figure 4b shows that, on the one hand, increasing the initial pressure from 50 to 200 Pa (respectively, 1000 Pa) obviously raises the CN density in the same ratio but without any influence on the $X_{CN}$ value; furthermore it

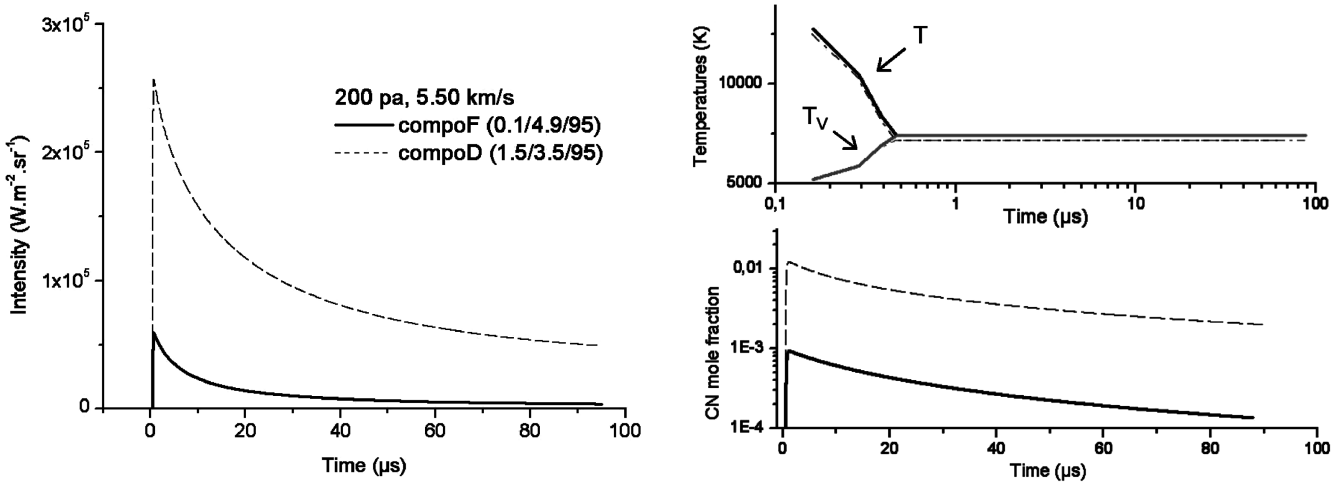


a) b)

**Fig. 3 Influence of large variations of $CH_4$ proportion on a) CN violet $\Delta v = 0$ time evolution, and b) temperatures $Tv$ (gray lines), $T$ (black lines), and CN mole fraction.**

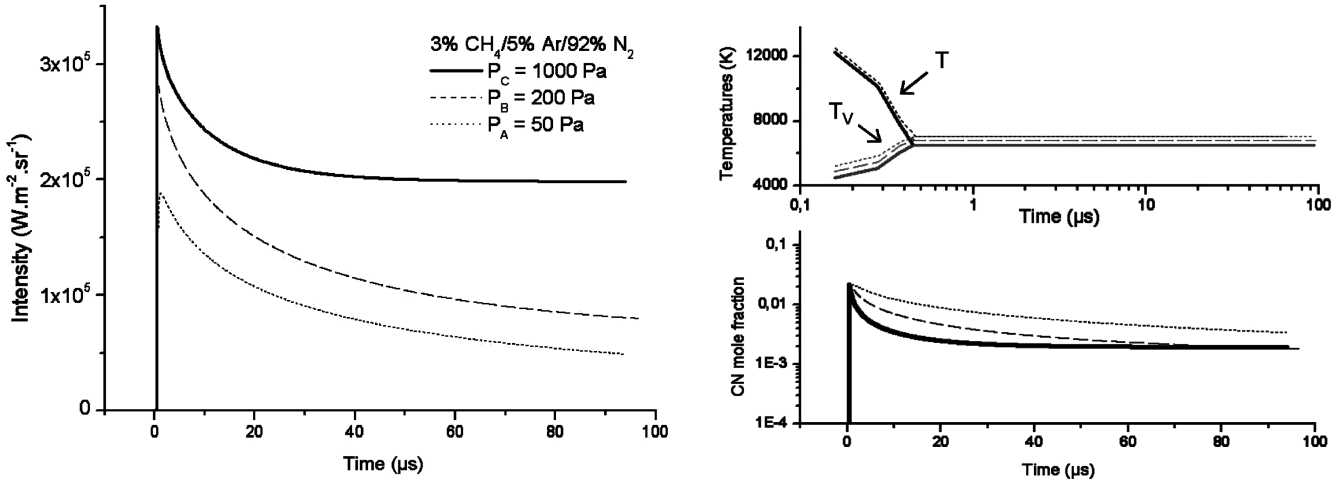


a) b)

**Fig. 4 Influence of large variations of the initial pressure on a) CN violet $\Delta v = 0$ time evolution, and b) temperatures $Tv$ (gray lines), $T$ (black lines), and CN mole fraction.**

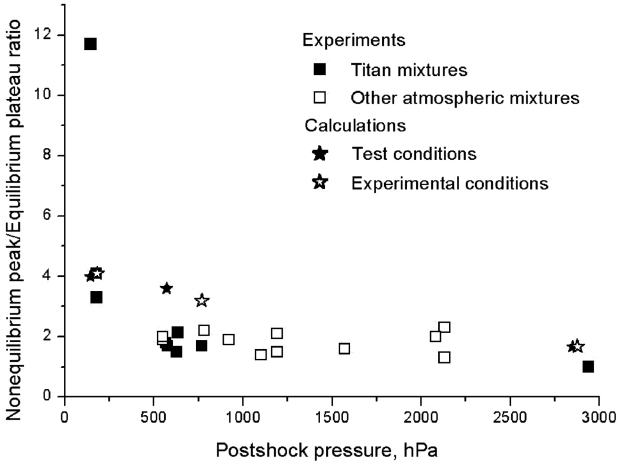


**Fig. 5 Relative extent of nonequilibrium and equilibrium fluxes with regard to the postshock pressure.**

brings about the growth of the vibrational temperature of 10% (16%). Because of these variations, the radiative flux increases by 50% (75%). On the other hand, the rise in pressure does not modify the vibrational temperature relaxation but the decay rate of the CN mole fraction is more rapid.

Experimental investigations showed the difference between energy radiated by the nonequilibrium and the equilibrium parts. Numerical estimations confirm the observed results: the lower the initial pressure, the higher the nonequilibrium emission. Figure 5, which represents the ratio between the nonequilibrium peak and the equilibrium plateau levels in relation to the postshock pressure, illustrates this behavior and shows that calculations agree well with experiments.

To sum up, the variation of the pressure has a direct consequence on CN density and consequently on the flux intensity. It also modifies the CN mole fraction evolution that changes on relaxation. The quantitative data are recapitulated in Table 4.

## IV. Comparisons with Experiments and Other Models

This section mainly deals with the comparison of experimental results obtained in Marseilles and presented in [15] with our numerical calculations based on a 2-$T$ model and Boltzmann radiation. The simulation of other experimental conditions completes the comparisons, namely, the Titan conditions of Bose et al. [11]. They performed their experiment in an electric arc-driven shock tube facility using monochromators coupled with photomultiplier tubes and spectrographs coupled with intensified CCD cameras.

For the Marseille experiments, we focus on two test conditions that were already simulated by SHOCK2 [30], a program based on the SHOCK code (CHEMKIN) [31] but modified into a 2-$T$ model, and PARADE, a line-by-line radiative code [32]. The obtained results, represented with dashed curves in Fig. 6, will be discussed in the next section. The TCM2 conditions and those of Bose et al. [11] simulated in this work are reported in Table 5.

### A. CN Violet System

Figure 6 represents the comparison between experimental results (black solid curves) and the numerical calculations of this work (gray solid curves) using Gökçen's kinetic scheme. The kinetic code is coupled with the radiative code PASTIS to obtain radiative results to make the comparison with experiments. Plots on the left column correspond to test case 1 (TC1) conditions, and the right column is for test case 2 (TC2). Figures 6a and 6b show the intensity profiles of the CN violet system ($\Delta v = 0$); spectra in Figs. 6c and 6d are extracted from 1 $\mu$s corresponding to the maximum of the time profiles; and spectra in Figs. 6e and 6f come from the attained equilibrium state.

Discrepancies are present between experiments and modeling. The numerical calculation overpredicts the radiative flux emitted behind the shock wave. The difference increases with the pressure: for high pressure, the emission during the first 35 $\mu$s is estimated numerically to be equal to 6 $\mathrm{J/m^2/sr}$ instead of 4 $\mathrm{J/m^2/sr}$ experimentally; and for low pressure the calculation gives about 3 $\mathrm{J/m^2/sr}$ and the experiment 1 $\mathrm{J/m^2/sr}$ during the first 20 $\mu$s. The simulation provides a good order of magnitude for the peak intensity and the level of equilibrium region agrees, but the relaxation is slower. The comparison of spectra also confirms these results; that is to say the computation of the nonequilibrium level is lightly higher and the intensity of the equilibrium zone matches.

The simulations of Bose et al. [11] conditions strengthen the two previous negative points. The calculations overestimate the radiative flux measured by the authors. But in this case, the main cause is the discrepancy with the equilibrium level that is not observed in the TCM2 study. The simulations largely overestimate the observed equilibrium intensity: for their three initial conditions the differences are bounded by 10 to 40. The flux of the peak is also slightly higher than experiment; for Figs. 6a–6c it is, respectively, calculated about 3, 2, and 2 times higher than measurements. Furthermore, the decay rate is numerically predicted as much slower.

The discrepancies between these radiative results could be explained by the differences in kinetic computations, particularly on the time evolution of CN mole fraction and temperatures. But unfortunately, neither CN mole fraction nor temperatures could be measured experimentally in the TCM2 shock tube campaign.

**Table 5 Experimental conditions**

| | $p_i$, Pa | $v_s$, km/s | $CH_4$–Ar–$N_2$, % |
|---|---|---|---|
| Test case 1 (TC1) | 211 | 5.62 | 95–2–3 |
| Test case 2 (TC2) | 50 | 5.50 | 95–2–3 |
| Bose et al. case a) [11] | 13.33 | 5.15 | 2–0–98 |
| Bose et al. case b) [11] | 13.33 | 5.56 | 5–0–95 |
| Bose et al. case c) [11] | 13.33 | 5.56 | 8.6–0–91.4 |

### B. Contribution of Main Radiative Systems

The radiative code PASTIS makes it possible to draw systems of various species from 100 to 1200 nm, in particular, CN and $C_2$ systems which are those observed experimentally. The coupling of our kinetic model and the PASTIS calculation for TC2 conditions provides the radiative flux evolution of CN red $\Delta v = +3$ and $C_2$ Swan $\Delta v = 0$. Figure 7 presents the comparison of the corresponding results with the experiments. For both systems the calculations overestimate the nonequilibrium radiative flux. $C_2$ Swan and CN red peaks are, respectively, predicted 3 and 40 times higher than experiments. As for CN violet, the CN red relaxation is calculated slower, whereas that of $C_2$ Swan is faster than experiments. The estimation of CN violet $\Delta v = 0$ is correct, but the high discrepancy occurring for the CN red $\Delta v = +3$ prediction invalidates the Boltzmann hypothesis.

Furthermore, with the PASTIS code the contribution of the whole CN violet, $C_2$ Swan, and CN red systems on the global radiative flux

**Table 4 Computed fluctuations of data in relation to the variations of the initial pressure**

| $P_1 \rightarrow P_2$, Pa | (Noneq./eq.) ratio $(I_{\mathrm{noneq}}/I_{\mathrm{eq}})_2/(I_{\mathrm{noneq}}/I_{\mathrm{eq}})_1$ | CN mole fraction ratio $(X_2/X_1)_{\mathrm{CN}}$ | $\frac{T_2-T_1}{T_1}$ | $\frac{\Phi_2-\Phi_1}{\Phi_1}$ |
|---|---|---|---|---|
| $50 \rightarrow 200$ | 0.93 | 1 | 10% | 50% |
| $50 \rightarrow 1000$ | 0.44 | 1 | 16% | 75% |

can be calculated. We experimentally estimated, for TC2 conditions, that the total energy density emitted during the first 20 $\mu$s is very close to 200 kJ/m$^2$/sr with 93% of CN violet, 4% of $C_2$ Swan, and 3% of CN red. Once again, Fig. 8 shows that the CN violet system is by far the main radiator in this range of wavelengths. In addition, band intensities of the CN red and $C_2$ Swan systems seem to be about 100 times lower. The CH A-X system does not appear contrary to what Hyun et al. [16] predicted for quite the same conditions.

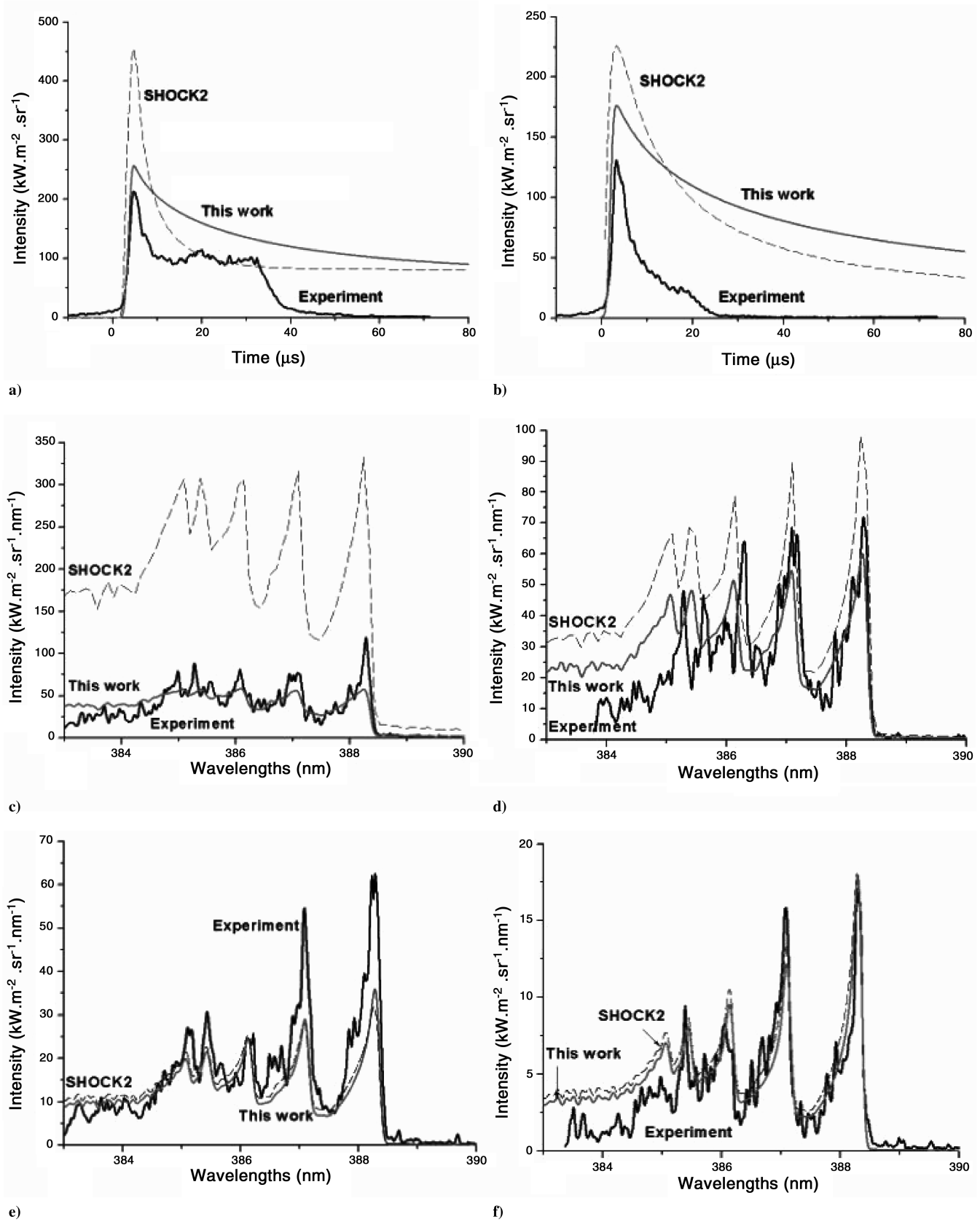


**Fig. 6 Comparisons between modeling and experimental time profiles a), b); spectra at the maximum intensity c), d); and equilibrium spectra e), f) of CN violet ($\Delta v = 0$) for two conditions: test case 1 a), c), and e) and test case 2 b), d), and f).**

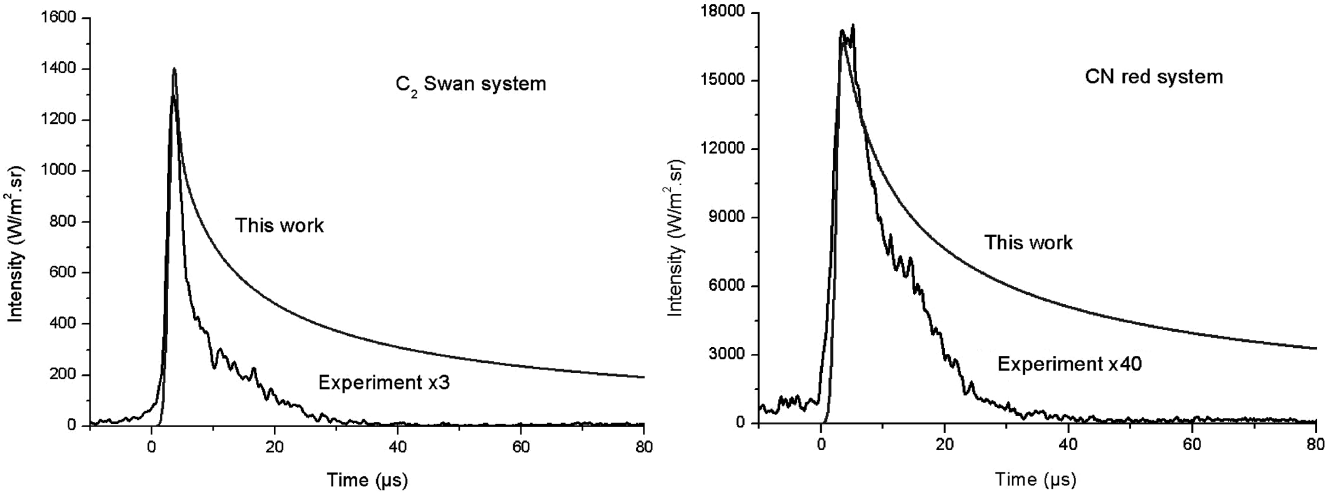


a) b)

**Fig. 7 Time evolution of the radiative flux in 3/2/95 mixture for $C_2$ Swan $\Delta v = 0$ ($p_i = 50$ Pa, $v_s = 5.45$ km/s) and CN red $\Delta v = +3$ ($p_i = 60$ Pa, $v_s = 5.58$ km/s).**

Quantitative results are summarized in Table 6 in terms of the flux ratio between systems.

Considering that these three systems are the only significant ones between 300 and 1200 nm, the total radiative flux calculated is composed of about 74% of CN violet, 25% of CN red, and 1% of $C_2$ Swan, which is very different from the experimental results (respectively, 93, 3, and 4%).

It is also interesting to compare both the $\Delta v = 0$ and $\Delta v = -1$ manifolds of the CN violet system. Experimental results [11,15] show that the intensity ratio $\Delta v = 0/\Delta v = -1$ of CN violet lies between 4 and 10, depending on the mixture and the pressure. Numerical simulations predict a lower rate equal to 2 at $P = 200$ Pa, 3.7 at $P = 50$ Pa, and 5 at $P = 40$ Pa. The ratio rises when the pressure decreases without following a linear law. The pressure drop goes together with the increase in vibrational temperature causing the high vibrational levels to overpopulate because of the Boltzmann hypothesis. So the self-absorption phenomenon becomes more significant for these high levels, reducing the intensity of manifolds $\Delta v = -1$ in relation to $\Delta v = 0$. The discrepancies between experiments and calculations come from an underestimation of self-absorption intensity because of an incorrect description of vibrational population distribution.

All these considerations on the discrepancy of the CN systems and manifolds ratio invalidate the hypothesis of the Boltzmann distribution on electronic and vibrational levels.

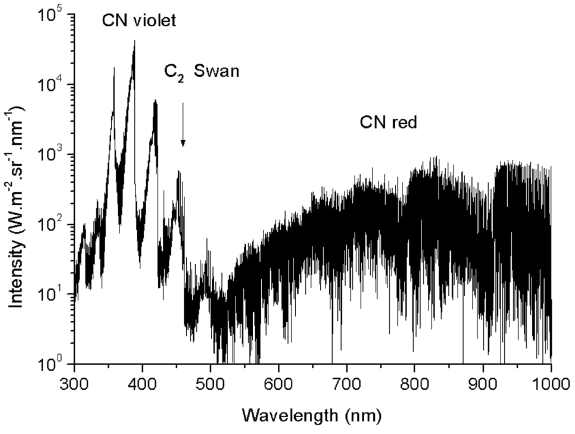


**Fig. 8 Global spectra corresponding to TC2 conditions during the nonequilibrium peak.**

## V. Comparisons with Other Models

### A. TCM2 Experimental Conditions

On top of the comparison between experimental results (solid black curves) and our simulation with the Gökçen kinetic scheme (solid gray curves), Fig. 6 also represents the SHOCK2 calculation using the Nelson kinetic scheme (dashed curves). Both kinetic codes were coupled with PASTIS to make the comparison with experiments.

#### *1. Radiative Results*

Discrepancies are present between both calculations. They estimate a close global flux on 100 $\mu$s (about 10 J/m$^2$/sr for TC1 and 7 J/m$^2$/sr for TC2) but the evolution of the emission does not correspond. The SHOCK2 calculation overestimates the intensity of the peak (nonequilibrium zone) but proposes a good simulation of the relaxation process; whereas our calculation provides a good order of magnitude for the peak intensity but the relaxation is slower. In both cases the intensity level of the equilibrium region agrees. The comparison of spectra confirms the previous results; that is to say, the nonequilibrium region is roughly simulated by SHOCK2 contrary to our calculations, and intensities of the equilibrium zone are in agreement.

#### *2. Kinetic Results*

To explain these discrepancies, the two thermochemical calculations are compared. Figure 9 represents the temperature evolution calculated by SHOCK2 and our model for TC1. We note that in the nonequilibrium zone, where SHOCK2 overestimates the flux, $(Tv)_{\text{shock2}}$ is higher than $(Tv)_{\text{this work}}$ and both $X_{\text{CN}}$ levels are close. The temperature relaxation process is faster for both calculations than experiment. But the $(X_{\text{CN}})_{\text{this work}}$ relaxation is slower than the SHOCK2 estimation as we observed that the decay rate for emissions was quite well simulated by SHOCK2 and slowly by this work. Finally, in the equilibrium part, where both simulations match, we note that temperatures from SHOCK2 are slightly lower than our calculation, but $X_{\text{CN}}$ is greater. So the equilibrium

**Table 6 Experimental and numerical contributions of main radiative systems**

| | Experiments results [15] | Numerical predictions |
|---|---|---|
| CN violet/$C_2$ Swan | 13 | 100 |
| CN violet/CN red | 35 | 3 |

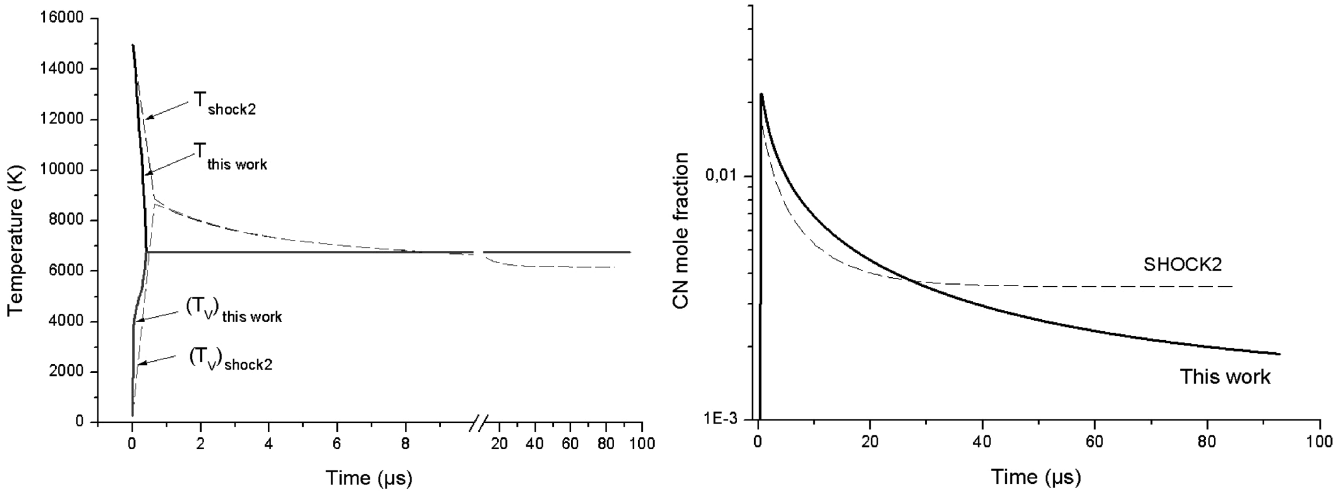


**Fig. 9 Comparisons between SHOCK2 (dashed lines) and this work (solid lines) modeling for TC1: a) $T$ and $Tv$; b) $X_{CN}$.**

calculation is correct, whereas numerical predictions fail for either nonequilibrium intensity or relaxation estimations.

As we observed for pressure influence results, the intensity of the radiative flux seems to be controlled mainly by the temperature, whereas the relaxation process is linked to the mole fraction evolution.

The experiments carried out on TCM2 with TC2 conditions were also simulated by Hyun et al. [16] for CN violet $\Delta v = 0$ and CN red $\Delta v = +3$ emission. Using a 2-$T$ model and the Boltzmann hypothesis they also overestimate the radiative flux by a factor of 10 for CN red emission and a factor of 5 for CN violet. Furthermore, the relaxation is calculated more slowly. Hyun et al. carry out another calculation using non-Boltzmann excitation with the radiation loss 6 times larger than that caused by CN violet and red systems. These results show agreement on the intensity and relaxation of CN violet, and on the decay rate of CN red, but do not improve the CN red intensity estimation.

### B. Bose et al. Conditions

To confirm these results, we performed a new numerical comparison between our calculations, and those of Bose et al. [11] and those of Hyun et al. [16] using the experimental conditions of the NASA Ames Research Center [cases a), b), and c)]. Whatever the group, the use of a Boltzmann distribution on CN excited states leads to an overestimation of the radiative flux and to estimate a slower rate of decay. We note that the predictions of the two other modelings are very close to each other, whereas our estimations are slightly lower.

Bose et al. [11] improves the simulations using a collisional radiative approach. The emission is then underestimated but there is no real influence on relaxation.

The SPRADIAN07 code of Hyun et al. [16] successfully reproduces the experimental data on CN radiation still making the hypothesis of a non-Boltzmann excitation, and the radiative power loss is multiplied by a factor of 6.

## VI. Conclusions

With regard to probe entries into the Titan atmosphere, two numerical codes are developed to simulate radiative processes occurring in shock tube experiments: a one-dimensional thermochemical calculation based on a two-temperature model and a line-by-line radiation code. The use of a simple physical model presents two interests: the investigation of the Gökçen chemical kinetic model on a 2-$T$ model and the enhancement of previous works applying different theories. We observe that using a 2-$T$ model decreases the computed ionization levels, as Gökçen predicted. We also have a slight influence on neutral species mole fractions, especially on hydride species. But one of the trickiest points concerning the physical calculation seems to be the uncertainty of thermodynamic parameters at high temperature. We want to emphasize this point which is usually not taken into account. We have to put into perspective the work on an accurate determination of kinetic reaction rates, whereas the results depend on the accuracy of thermodynamic data.

Obviously it is also of great interest to study the influence of the chemical kinetic model on calculations. The improvement introduced by the use of Gökçen's more detailed kinetic model in relation to Nelson's short model is confirmed, particularly on methane decomposition which plays an important role in CN formation.

The analysis of some key-parameter sensitivity highlights their relative influence on radiative flux. The low variations in gas composition, initial pressure, and shock velocity has no influence on the radiative heat flux. These results make the comparison between experiments relevant in spite of the experimental uncertainty and the rough reproducibility. On the other hand, wide variations are significant for $CH_4$ and the initial pressure. The negligible proportion of $CH_4$ in the mixture is responsible for the small amount of formed CN and thus for the weak emission of its violet system. In agreement with experiments, we note that the rise of the initial pressure causes the increase of this emission, because of the growth of CN density, a faster relaxation due to the faster return to equilibrium of the CN mole fraction, and the reduction in the emission of the nonequilibrium region in relation to the equilibrium one.

The comparisons of experimental results from TCM2 runs and Bose et al. [11] using different numerical simulations confirm that results are sensitive to both chemical and physical implemented models. Most of the results presented in this paper lead us to think that, for the 2-$T$ model, the intensity of the radiative flux is controlled mainly by the temperature, whereas the relaxation process is linked to the mole fraction evolution. The Boltzmann distribution assumption for the CN excited states leads systematically to the overprediction of the intensity. This hypothesis does not lend itself to a precise description of the thermochemical evolution of the gas behind a strong shock wave. Furthermore, the discrepancies in the contributions of main radiative systems all invalidate the Boltzmann equilibrium hypothesis and so constitute arguments in favor of a collisional radiative model. Lastly, the results of Hyun et al. [16] speak in favor of the insertion of radiative processes into the thermochemical code to take into account the radiative power loss. The development of detailed calculations is of great interest to describe the physical and chemical processes. But, currently, the time cost of these calculations remains too high and they do not provide significant improvement of radiative flux estimation in relation to 2-$T$ calculations. For these reasons it is not relevant to couple this kind of algorithm with computational fluid dynamics codes.

## Acknowledgments

The authors wish to express their thanks to Arnaud Bultel from the University of Rouen for numerous discussions and to Dawn Hallidy from the University of le Havre for his valuable comments.

## References

[1] Lebreton, J. P., Witasse, O., Sollazzo, C., Blancquaert, T., Couzin, T., Schipper, A.-M., Jones, J. B., Matson, D. L., Gurvits, L. I., Atkinson, D. H., Kazeminejad, B., and Pérez-Ayucar, M., "An Overview of the Descent and Landing of the Huygens Probe on Titan," *Nature (London)*, Vol. 438, Dec. 2005, pp. 758–764. doi:10.1038/nature04347

[2] Matson, D. L., Spilker, L. J., and Lebreton, J.-P., "The Cassini-Huygens Mission to the Saturnian System," *Space Science Reviews*, Vol. 104, Nos. 1–4, July 2002, pp. 1–58. doi:10.1023/A:1023609211620

[3] Lebreton J.-P., and Matson, D. L., "The Huygens Probe: Science, Payload and Mission Overview," *Space Science Reviews*, Vol. 104, Nos. 1–4, July 2002, pp. 59–100. doi:10.1023/A:1023657127549

[4] Park, C., "Radiation Enhancement by Nonequilibrium During Flight Through the Titan Atmosphere," AIAA Paper 82-0878, 1982.

[5] Bershder, D., and Park, C. S., "Nonequilibrium Shock Layer Radiation in a Simulated Titan Atmosphere," *International Workshop on Strong Waves*, edited by H. Honma and K. Maeno, Seichosha, Tokyo, 1992.

[6] Park, C., "Problems of Rate Chemistry in the Flight Regimes of Aeroassisted Orbital Transfer Vehicles," AIAA Paper 84-1730, 1984.

[7] Gökçen, T., "$N_2$-$CH_4$-Ar Chemical Kinetic Model for Simulations of Titan Atmospheric Entry," *Journal of Thermophysics and Heat Transfer*, Vol. 21, No. 1, 2007, pp. 9–18. doi:10.2514/1.22095

[8] Jaffe, R. L., "Rate Constants for Chemical Reactions in High-Temperature Nonequilibrium Air," AIAA Paper 85-1038, 1985.

[9] Nelson, H. F., Park, C., and Whiting, E. E., "Titan Atmospheric Composition by Hypervelocity Shock Layer Analysis," *Journal of Thermophysics and Heat Transfer*, Vol. 5, No. 2, 1991, pp. 157–165. doi:10.2514/3.243

[10] Lee, J. H., "Basic Governing Equations for AOTV Flight Regimes," AIAA Paper 84-1729, 1984.

[11] Bose, D., Wright, M. J., Bogdanoff, D. W., Raiche, G. A., and Allen, G. A., "Modeling and Experimental Validation of CN Radiation Behind a Strong Shock Wave," AIAA Paper 2005-768, 2005.

[12] Magin, T. E., Caillault, L., Bourdon, A., and Laux, C. O., "Nonequilibrium Radiation Modeling for Huygens Entry," *3rd International Planetary Probe Workshop*, 2005.

[13] Johnston, C. O., Hollis, B. R., and Sutton, K., "Radiative Heating Methodology for the Huygens Probe," AIAA Paper 2006-3426, 2006.

[14] Osawa, H., Matsuyama, S., Ohnishi, N., and Sawada, K., "Comparative Computation of Radiative Heating Environment for Huygens Probe Entry Flight," AIAA Paper 2006-3772, 2006.

[15] Rond, C., Boubert, P., Felio, J. M., and Chikhaoui, A., "Radiation Measurements in a Shock Tube for Titan Mixtures," *Journal of Thermophysics and Heat Transfer*, Vol. 21, No. 3, 2007, pp. 638–646. doi:10.2514/1.28422

[16] Hyun, S.-Y., Park, C., and Chang K.-S., "Rate Parameters for Electronic Excitation of Diatomic Molecules, 3. CN Radiation Behind a Shock Wave," AIAA Paper 2008-1276, 2008.

[17] Yelle, R. V., Strobell, D. F., Lellouch, E., and Gautier, D., "Engineering Models for Titan's Atmosphere," ESA SP-1177, European Space Agency, Noordwijk, 1997.

[18] Candler, G. V., and MacCormack, R. W., "The Computation of Hypersonic Ionized Flows in Chemical and Thermal Nonequilibrium," AIAA Paper 88-0511, 1988.

[19] Park, C., "Assessment of Two-Temperature Kinetic Model for Ionizing Air," *Journal of Thermophysics and Heat Transfer*, Vol. 3, No. 3, 1989, pp. 233–244. doi:10.2514/3.28771

[20] Gnoffo, P. A., Gupta, R. N., and Shinn, J. L., "Conservation Equations and Physical Models for Hypersonic Air Flows in Thermal and Chemical Nonequilibrium," NASA TP 2867, 1989.

[21] Park, C., *Nonequilibrium Hypersonic Aerothermodynamics*, Wiley, New York, 1990.

[22] Park, C., "Assessment of Two-Temperature Kinetic Model for Dissociating and Weakly-Ionizing Nitrogen," AIAA Paper 86-1347, 1986.

[23] Millikan, R. C., and White, D. R., "Systematics of Vibrational Relaxation," *Journal of Chemical Physics*, Vol. 39, No. 12, 1963, pp. 3209–3213. doi:10.1063/1.1734182

[24] Marrone, P. V., and Treanor, C. E., "Chemical Relaxation with Preferential Dissociation from Excited Vibrational Levels," *Physics of Fluids*, Vol. 6, No. 9, 1963, pp. 1215–1221. doi:10.1063/1.1706888

[25] Gordon, S., and McBride, B. J., "Computer Program for Calculation of Complex Chemical Equilibrium Compositions and Applications," NASA RP 131, 1994.

[26] NASA Glenn Research Center, http://cea.grc.nasa.gov/.

[27] Capitelli, M., Colonna, G., Giordano, D., Marraffa, L., Casavola, A., Minelli, P., Pagano, D., Pietanza, L. D., and Taccogna, F., Tables of Internal Partition Functions and Thermodynamic Properties of High-Temperature Mars-Atmosphere Species From 50 K to 50000 K, ESA Publications Division, ESTEC, Noordwijk, The Netherlands, 2005.

[28] William, J., "Etude des Processus Physico-Chimiques Dans les Ecoulements Détendus à Haute Enthalpie: Application à la Soufflerie à Arc F4," Ph.D. Thesis, Université de Provence, France, 1997.

[29] Boubert, P., and Vervisch, P., "CN Spectroscopy and Physico-Chemistry in the Boundary Layer of a C/SiC Tile in a Low Pressure Nitrogen/Carbon Dioxide Plasma Flow," *Journal of Chemical Physics*, Vol. 112, No. 23, 2000, pp. 10482–10490. doi:10.1063/1.481682

[30] Mazoué, F., "Huygens Probe Entry into Titan Atmosphere. Heat Fluxes Studies," ESA Technical Report, 2004.

[31] Kee, R. J., Rupley, F. M., and Miller, J. A., "CHEMKIN II: A Fortran Chemical Kinetics Package for the Analysis of Gas-Phase Chemical Kinetics," Sandia National Laboratories SAND89-8009, Livermore, CA, 1989.

[32] Smith, A. G., Gogel, T., Vandevelde, P., and Marraffa, L., "Plasma Radiation Database PARADE Final Report," ESTEC Contract 11148/94/NL/FG, 1996.